Supporting Information

The Role of Pre-Defined Microporosity in Catalytic Site Formation for Oxygen Reduction Reaction in Iron- and Nitrogen-Doped Carbon Materials

Minhyoung Kim,[‡ab] Hee Soo Kim,[‡c] Sung Jong Yoo,[de] Won Cheol Yoo*[cf] and Yung-Eun Sung*[ab]

[a] Center for Nanoparticle Research, Institute for Basic Science (IBS), Seoul 08826, Republic of Korea. *E-mail: ysung@snu.ac.kr

[b] School of Chemical and Biological Engineering, Seoul National University, Seoul 08826, Republic of Korea.

[c] Department of Applied Chemistry, Hanyang University, Ansan 15588, Republic of Korea. *E-mail: wcyoo@hanyang.ac.kr

[d] Fuel Cell Research Center, Korea Institute of Science and Technology (KIST), Seoul 02792, Republic of Korea.

[e] Clean Energy and Chemical Engineering, Korea University of Science and Technology, Daejeon 34113, Republic of Korea.

[f] Department of Chemical and Molecular Engineering, Hanyang University, Ansan 15588, Republic of Korea.
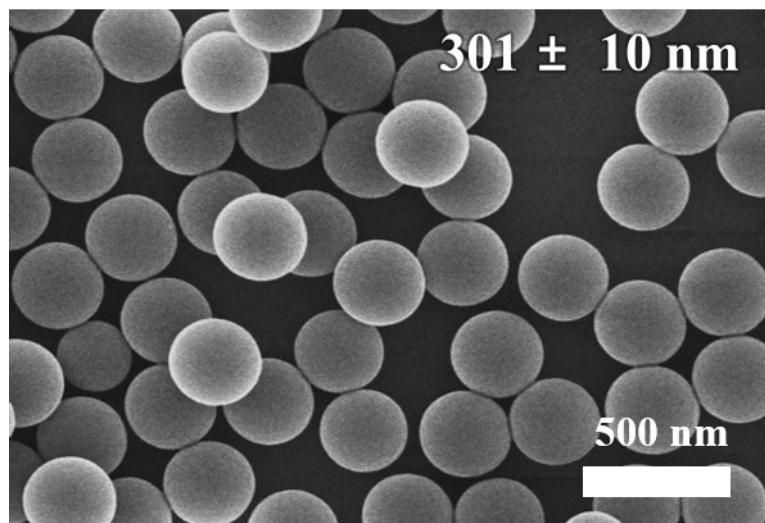
Fig. S1. SEM images of the RFP sample.

(a) RFC 206 ± 10 nm 500 nm

(b) RFC_C30 196 ± 14 nm 500 nm

(c) RFC_C120 179 ± 19 nm 500 nm

(d) RFC_C240 163 ± 23 nm 500 nm
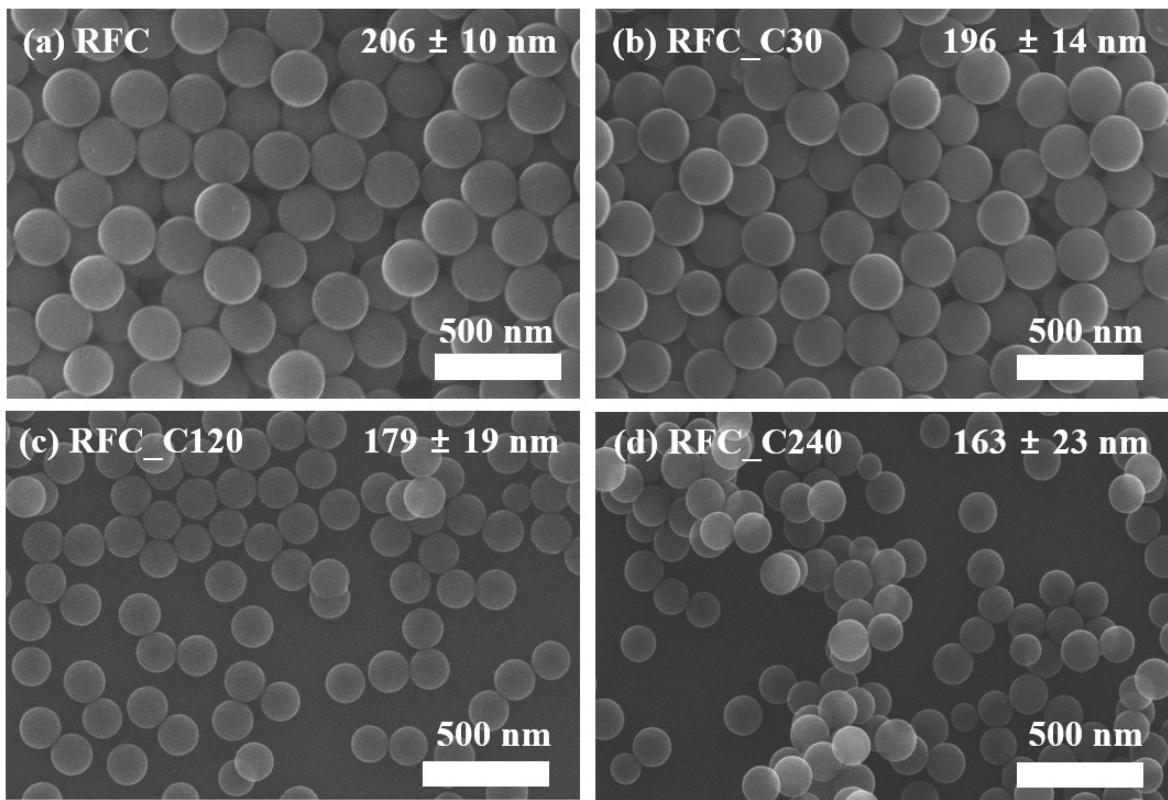
**Fig. S2.** SEM images of the RFC_CX series.
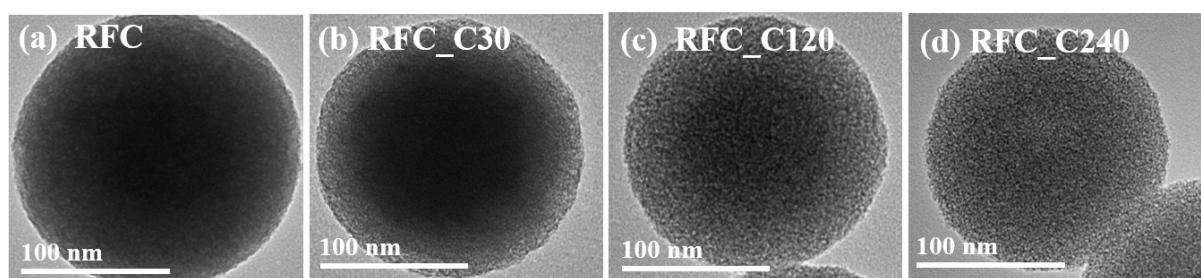
**Fig. S3.** TEM images of the RFC_CX series.
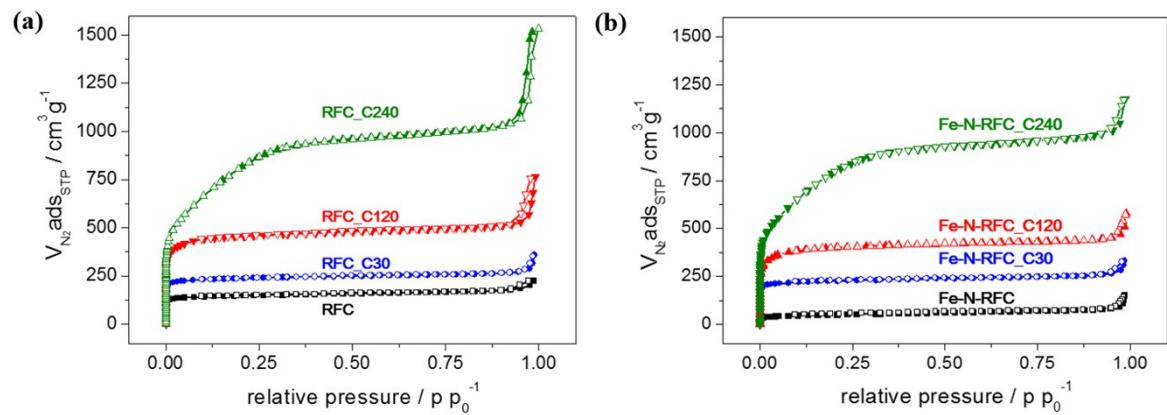
Fig. S4. Nitrogen adsorption-desorption isotherms for (a) RFC_CXs and (b) Fe-N-RFC_CXs.
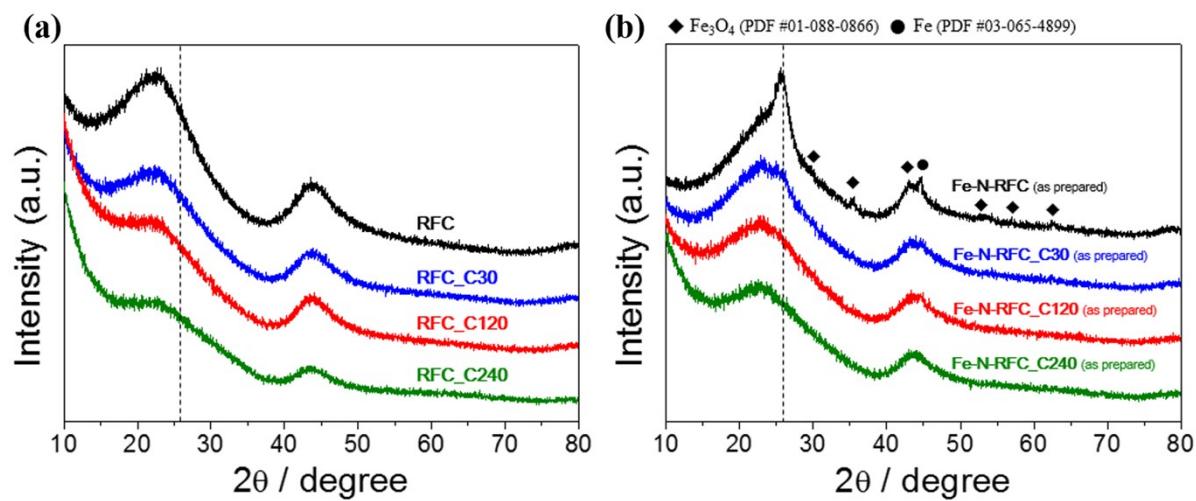
Fig. S5. XRD patterns for (a) RFC_CX and (b) as-prepared Fe-N-RFC_CX; before acid leaching step.
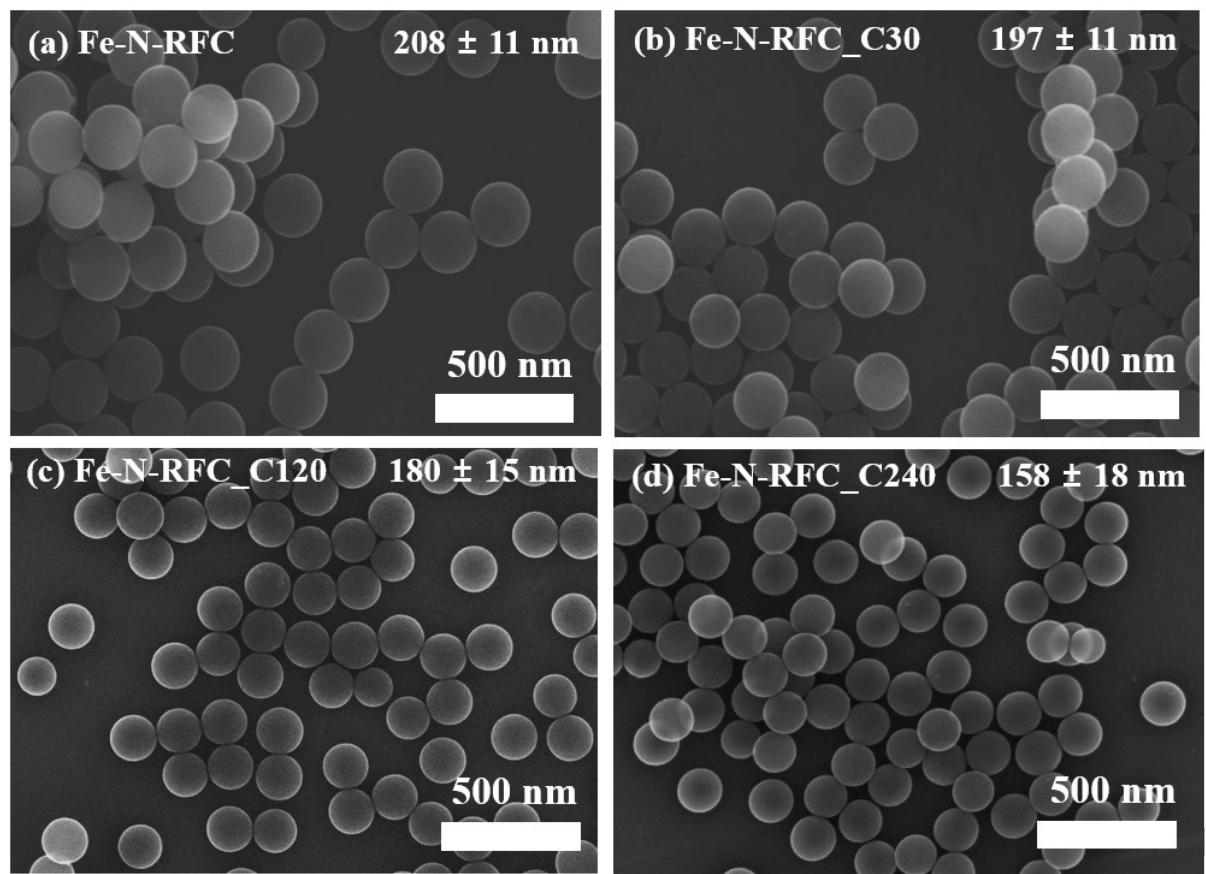
**Fig. S6.** SEM images of the Fe-N-RFC_CX series.
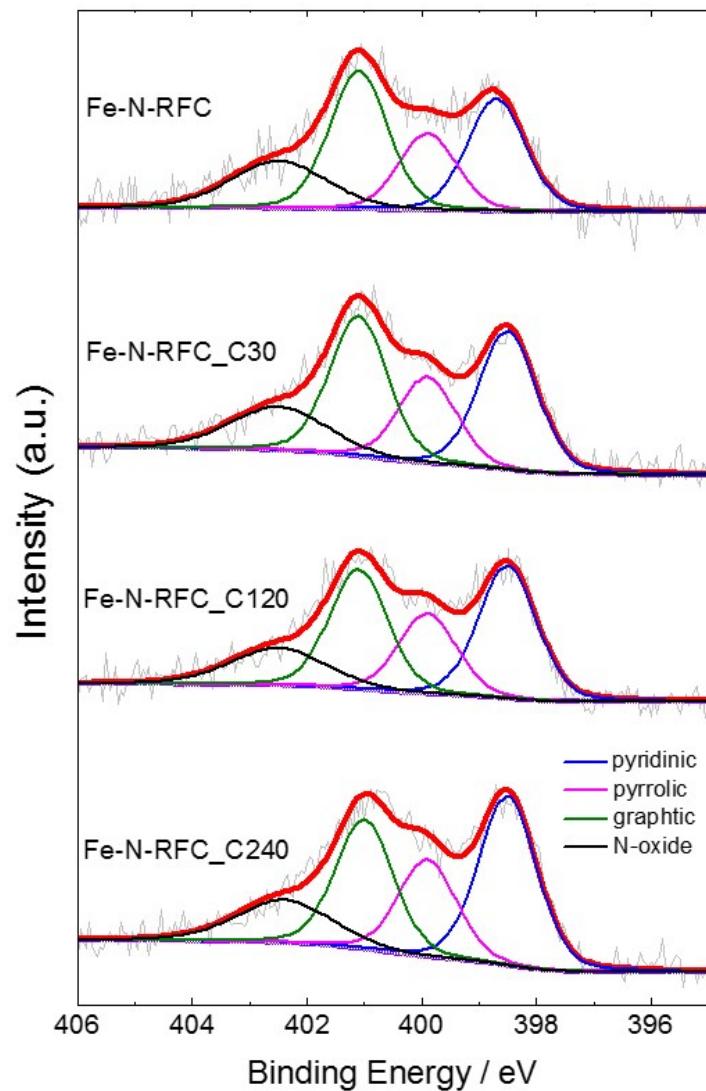
Fig. S7. XPS N1s peaks and fitting results for Fe-N-RFC_CX samples.
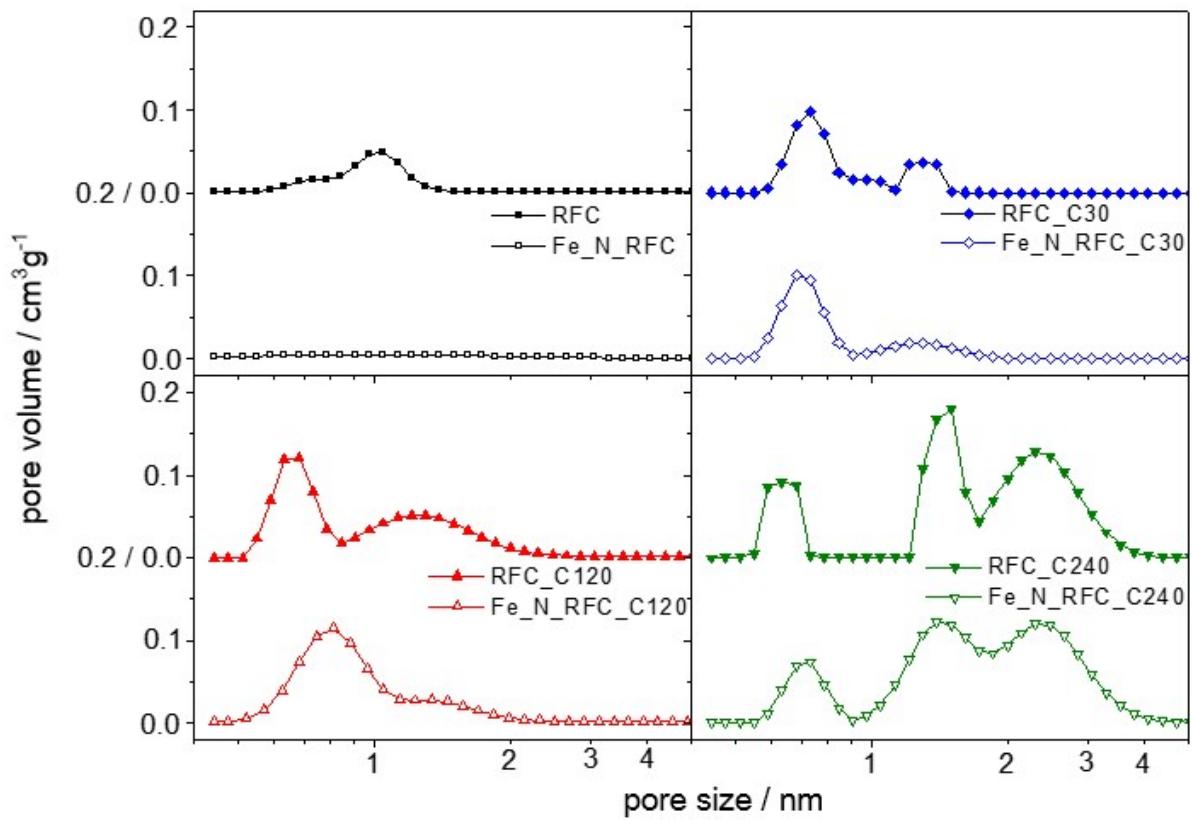
Fig. S8. Comparative BET isotherm analyses on incremental pore volume as the function of pore size in samples before/after Fe-N-doping process
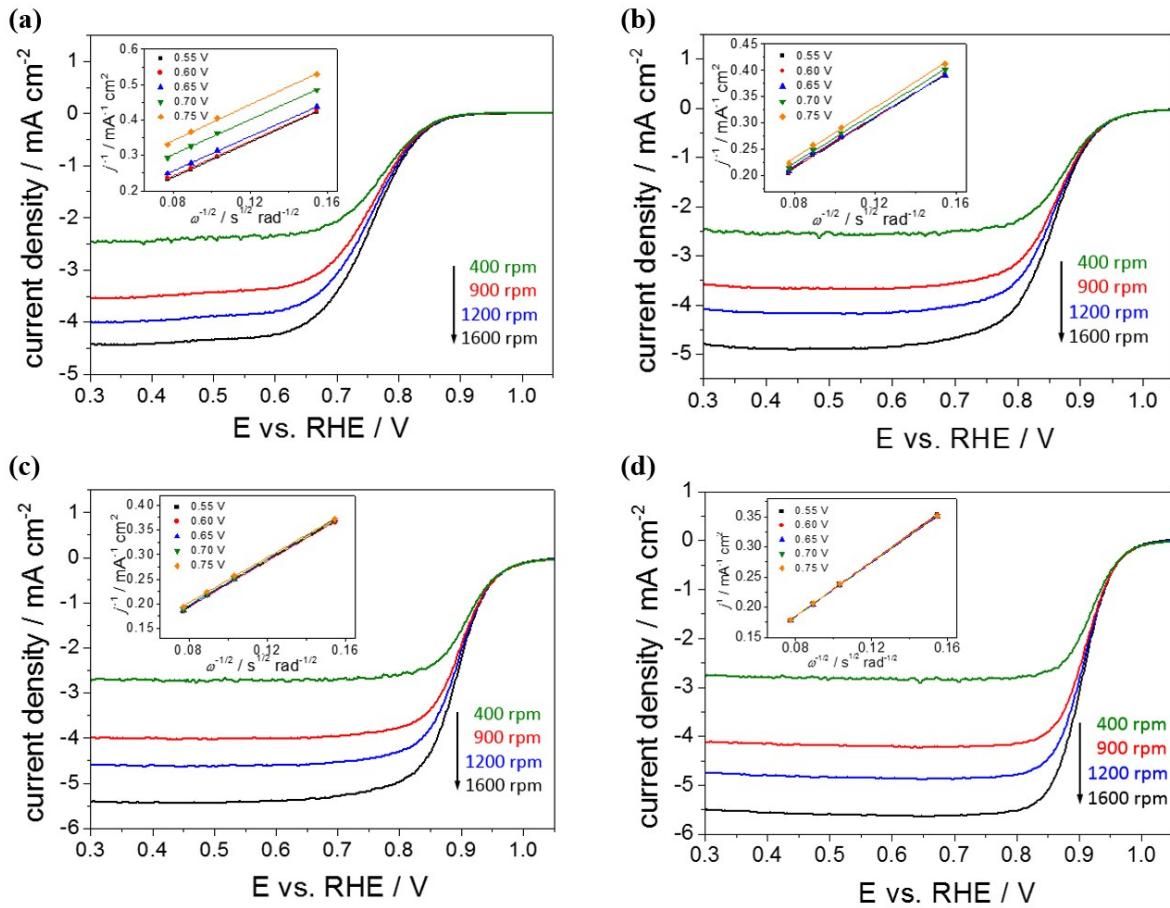
Fig. S9. RDE polarization curves for (a) Fe-N-RFC (b) Fe-N-RFC_C30 (c) Fe-N-RFC_C120 and (d) Fe-N-RFC_C240 in O_2-saturated 0.1 M KOH at a scan rate of 5 mV sec^{-1} with various electrode rotating rates (inset) Koutecky-Levich plot of J^{-1} vs $\omega^{1/2}$ at 0.55, 0.60, 0.65, 0.70 and 0.75 V vs RHE.
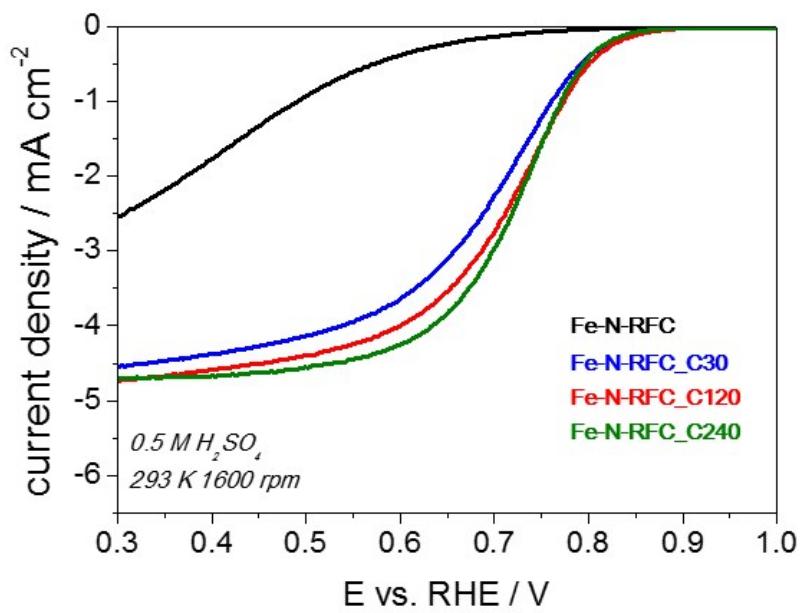
Fig. S10. RDE polarization curves of Fe-N-RFC_CX in O_2-saturated 0.5 M H_2SO_4 with a scan rate of 5 mV sec^{-1}, 1600 rpm
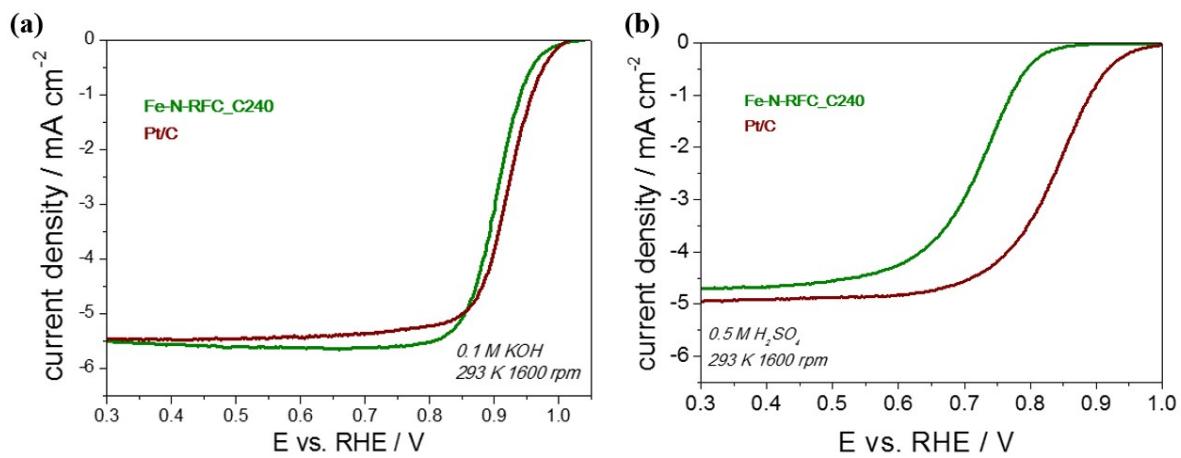
Fig. S11. RDE polarization curves of Fe-N-RFC_C240 and commercial Pt/C 20wt% catalyst in O_2-saturated (a) 0.1 M KOH and (b) 0.5 M H_2SO_4. Pt loading: 0.06 mg cm^{-2}.

Sample	relative N site (%)			
	pyridinic	pyrrolic	graphitic	N-oxide
Fe-N-RFC	27.7	18.9	34.0	19.4
Fe-N-RFC_C30	31.7	19.7	32.0	16.6
Fe-N-RFC_C120	33.6	20.3	30.3	15.8
Fe-N-RFC_C240	36.2	20.8	27.8	15.2

Table S1. Relative N sites for Fe-N-RFC_CXs from the fitting results of XPS N1s peaks

Catalysts	Loading amounts (mg cm-2)	Half-wave potential (V vs. RHE)	On-set potential (V vs. RHE)	Rotating speed (rpm)	Reference
Co$_3$O$_4$/N-rmGO	0.10	0.83	ca. 0.90	1600	1
NG/Fe$_{5.0}$	0.05	-	-0.04 V (vs. Ag/AgCl)	1600	2
FePc-Py-CNTs	0.32	0.915	-	-	3
N-Fe-CNT/CNP	0.20	0.87±0.01	0.99	900	4
	1.00	0.93	1.05		
Fe3C/C-800	0.60	0.83	1.05	900	5
Fe-N/C-800	0.10	0.809	0.923	1600	6
Fe-PANI/C-Mela	0.51	0.88	1.01	1600	7
C-COP-P-Co	0.20	ca. 0.80	-	1600	8
CNPs	0.39	0.92	1.03	900	9
carbon nanoshell	0.10	0.85	0.98	1600	10
Fe-N-CNFs	0.60	0.81	0.93	1600	11
GF+N2+Fe1_800	0.10	0.846	0.907	1600	12
CoO$_x$/Co@GC-NC	-	0.858	0.974	1600	13
Fe-N-RFC_C240	0.50	0.91	0.998	1600	This work

Table S2. Summary of reported ORR performance for Fe-N-C catalysts in 0.1 M KOH.

References

1   Y. Liang, Y. Li, H. Wang, J. Zhou, J. Wang, T. Regier, H. Dai, *Nat. Mater.*, 2011, **10**, 780-786.
2   K. Parvez, S. Yang, Y. Hernandez, A. Winter, A. Turchanin, X. Feng, K. Müllen, *ACS Nano*, 2012, **6**, 9541-9550.
3   R. Cao, R. Thapa, H. Kim, X. Xu, M. G. Kim, Q. Li, N. Park, M. Liu, J. Cho, *Nat. Commun.*, 2013, **4**, 2076.
4   H. T. Chung, J. H. Won, P. Zelenay, *Nat. Commun.*, 2013, **4**, 1922.
5   Y. Hu, J. O. Jensen, W. Zhang, L. N. Cleemann, W. Xing, N. J. Bjerrum, Q. Li, *Angew. Chem. Int. Ed.*, 2014, **53**, 3675-3679.
6   L. Lin, Q. Zhu, A.-W. Xu, *J. Am. Chem. Soc.*, 2014, **136**, 11027-11033.
7   H. Peng, F. Liu, X. Liu, S. Liao, C. You, X. Tian, H. Nan, F. Luo, H. Song, Z. Fu, *ACS Catal.*, 2014, **4**, 3797-3805.
8   Z. Xiang, Y. Xue, D. Cao, L. Huang, J. F. Chen, L. Dai, *Angew. Chem. Int. Ed.*, 2014, **53**, 2433-2437.
9   S. Zhao, H. Yin, L. Du, L. He, K. Zhao, L. Chang, G. Yin, H. Zhao, S. Liu, Z. Tang, *ACS Nano*, 2014, **8**, 12660-12668.
10 Y. Wang, A. Kong, X. Chen, Q. Lin, P. Feng, *ACS Catal.*, 2015, **5**, 3887-3893.
11 Z. Y. Wu, X. X. Xu, B. C. Hu, H. W. Liang, Y. Lin, L. F. Chen, S. H. Yu, *Angew. Chem.*, 2015, **127**, 8297-8301.
12 K. Qiu, G. Chai, C. Jiang, M. Ling, J. Tang, Z. X. Guo, *ACS Catal.*, 2016, **6**, 3558-3568.
13 J. Yu, G. Chen, J. Sunarso, Y. Zhu, R. Ran, Z. Zhu, W. Zhou, Z. Shao, *Advanced Science*, 2016, DOI: 10.1002/advs.201600060.